Article:

Sizling, AL, Sizlingova, E, Tjorve, E et al. (2 more authors) (2017) How to allow SAR collapse across local and continental scales: a resolution of the controversy between Storch et al. (2012) and Lazarina et al. (2013). Ecography, 40 (8). pp. 971-981. ISSN 0906-7590

https://doi.org/10.1111/ecog.02181

On Line Supplementary Information

to

An analytical resolution of the controversy between Storch et al. (2012) and Lazarina et al. (2013)

by

Arnošt Leoš Šizling[1], Eva Šizlingová[1], Even Tjørve[2], Kathleen M.C. Tjørve[2], William E. Kunin[3]

[1]Center for Theoretical Study, Charles University in Prague, Czech Republic; [2]Lillehammer University College, Norway;

[3]School of Biology, University of Leeds, United Kingdom

Content

SI-1: Derivation of the Eq. 3

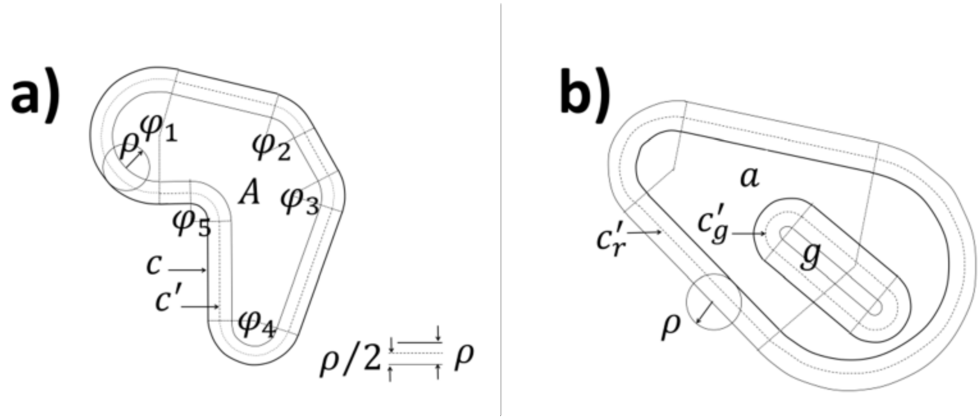

Here we show that the difference between c' (c'_r, c'_g) and c (c_r, c_g) can be approached by $2\pi\rho$, where ρ is the radius of the sample plot. The figure shows a geometric model of arena (a) and range including gap (b) of the 'real' shapes of the arena and range in Fig. 1. The notation and meaning of the lines (bold, thin, dashed) follows the capture of the Fig. 1. Dotted lines delimit the arcs that serve as the corners of the arena, gap and range. These lines are perpendicular to the respective lines that serves as the linear parts of the edges; therefore only changes in the arcs lengths contribute to the differences between c' and c. The length of each arc is given by '$\varphi \cdot q$' where φ is an angle of the arc (in radians) and q is the arc radius. Each arc that makes a corner is thus shorter by $\varphi \cdot q - \varphi \cdot (q - \rho/2) = \varphi \cdot \rho/2$ or longer by $\varphi \cdot (q + \rho/2) - \varphi \cdot q = \varphi \cdot \rho/2$. The change in the corner length is therefore independent from its radius, which vary between the corners. For the convex corners (φ_1 ... φ_4), the change is positive, and for concave corners (φ_5) is the change negative. Because the shape is given by a closed limit (its limit delimits a finite area) the sum across all corners makes the whole circle and thus $\left(\sum \varphi_i - \sum \varphi_j\right) \cdot \rho/2 = 2\pi \cdot \rho/2 = \pi \cdot \rho$, where the first and second summations run across the convex and concave corners, respectively. The same applies for the range and gaps. In sake of simplicity, we did not put symbols φ for angles into (b) and q for diameters into (a,b).

SI-2: Derivation of FAE

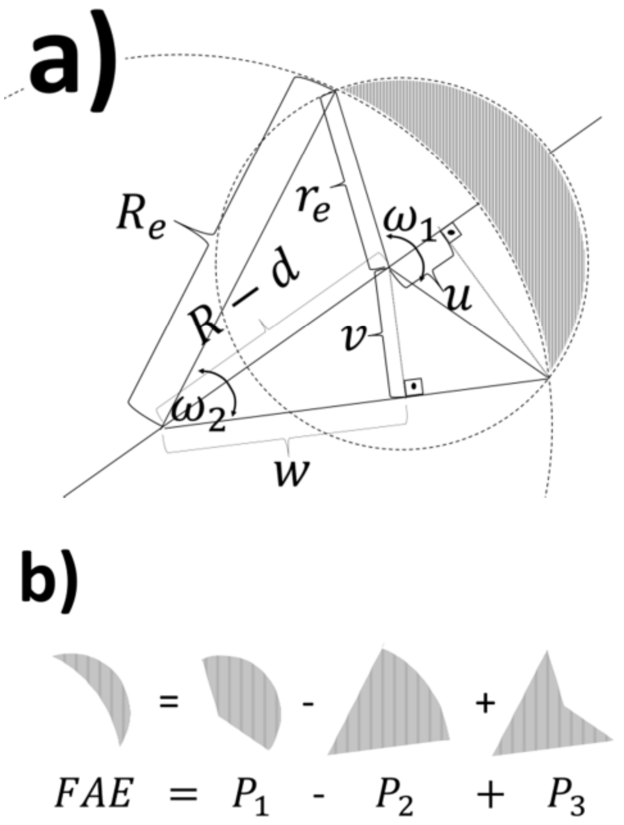

FAE is estimated as the moon shaped filled area (a) in our approach. Dashed circles show the effective arena (radius R_e) and the effective range (radius r_e). R is the virtual radius of the range and d is distance of the range centre from the edge of the arena. The angles ω_{1-2} delimit the respective parts of the circular approaches to the arena and range. The figure b shows the computation of FAE. FAE be computed as the part of the range that is delimited by ω_1 minus the part of the arena that is delimited by the angle ω_2 plus the two triangles that are taken from the arena. The three light grey areas in (b) correspond to the three additive terms in the Eq. 10.

$P_1 = \frac{1}{2} R_e^2 \cdot \omega_1$ where $\cos\frac{\omega_1}{2} = \frac{u}{r_e}$ where u originates as the solution of the equation $\frac{R-d+u}{R_e} = \frac{w}{R-d}$ which is a simple consequence of similarity between the triangles with shared angle $\omega_1/2$ and edges w and R_e. The value of w is given by the solution of system of two equations: (i) $w^2 + v^2 = (R-d)^2$, and (ii) $(R_e - w)^2 + v^2 = r_e^2$. These equations are Pythagoras theorems for the particular triangles.

$P_2 = \frac{1}{2} r_e^2 \cdot \omega_2$ where $\cos\frac{\omega_2}{2} = \frac{w}{R-d}$.

$P_3 = v \cdot R_e$ where v is the solution of the above equations (e.g., $v^2 = r_e^2 - (R_e - w)^2$).

FAE (Eq. 10) is made then by solving the above equations and summing $P_1 - P_2 + P_3$.

The above computation of FAE has its limits. If the effective range (small circle) is too small to intersect the edge of effective arena (the big circle), than there is no moon shaped area and FAE=0. On the other hand, if the $r + \rho$ is so large that the circle with this radius encompass the effective range, there is also no moon shaped FAE and FAE is made by the circle with radius $r + \rho$ minus the effective arena.

In the first case, the condition is given by inequality $r_e < R_e - (R - d)$ (see Fig. SI-2a), which can be expanded as $r + \rho < d - \rho$. It follows $\rho < (d - r)/2$, which is $\sigma < \sigma_{min} = \pi\,(d - r)^2/4$ in terms of range and sample areas. The σ_{min} is the finest scale at which the Finite Area Effect occurs.

In the second case, the condition is given by inequality $r_e > R - d + R_e$ (see Fig. SI-2a), which can be expanded as $r + \rho > 2R - d - \rho$. It follows $\rho > (2R - d - r)/2$, which is $\sigma > \sigma_{sat} = \pi\,(2R - r - d)^2/4$ in terms of range and sample areas. The σ_{sat} is the area of saturation (Šizling and Storch 2004), i.e., the scale at which the Finite Area Effect saturates.

In more technical language, $\mathrm{FAE}(\sigma) = 0,$ where $\sigma \le \sigma_{min}$; $\mathrm{FAE}(\sigma) = P_1 - P_2 + P_3$ (Eq. 10) where $\sigma_{min} \le \sigma \le \sigma_{sat}$; and $\mathrm{FAE}(\sigma) = \pi\left(r_{e,i}^2 - R_e^2\right) = a - A + 2\left(\sqrt{a} - \sqrt{A}\right)\sqrt{\sigma}$ where $\sigma_{sat} \le \sigma$.

SI-3: Slope (derivative) of rescaled SAR

$Slope = \frac{\partial \ln S^*(\sigma^*)}{\partial \ln \sigma^*} = \frac{1}{S^*(\sigma^*)} \frac{\partial S^*(\sigma^*)}{\partial \sigma^*} \frac{d e^{ln\sigma^*}}{d ln\sigma^*} = \frac{\sigma^*}{S^*(\sigma^*)} \frac{\partial S^*(\sigma^*)}{\partial \sigma^*}$. It follows the Eq. 27 where

$K_1 = \frac{\partial \mathrm{FAE}'_{tot}(\sigma^*)}{\partial \sigma^*} \sigma^{*2.5} - C'_1 \sigma^{1.5} + (C'_1 - C'_2/2)\sigma^* + \left(C'_2 - \mathrm{FAE}'_{tot}(\sigma^*)\right)\sigma^{*0.5} + C'_3$,

$K_2 = -\sqrt{A}\left(\frac{\partial \mathrm{FAE}'_{tot}(\sigma^*)}{\partial \sigma^*} \sigma^{*2} - C'_1 \alpha^* - \frac{C'_2}{2} \sigma^{*0.5}\right)$, $K_3 = -C'_1 \sigma^{*1.5} - C'_2 \sigma^* + (\mathrm{FAE}'_{tot}(\sigma^*) - C'_3)\sigma^{*0.5}$, and

$K_4 = \sqrt{A}\left(C'_1 \sigma^* + C'_2 \sigma^{*0.5} + C'_3 - \mathrm{FAE}'_{tot}(\sigma^*)\right)$.

The coefficients C'_{1-3} are standardized coefficients C_{1-3} (Eqs. 18-20) devided by A, i.e., $C'_1 = C_1/A$; $C'_2 = C_2/\left(A\sqrt{\bar{a}}\right)$; and $C'_3 = C_3/(A \cdot \bar{a})$.

When we fitted the Eq. 27 to the data extracted from Storch et al. (2012) and Lazarina et al. (2013), we assumed an independency of the coefficients K_{1-4} and FAE from σ^*. This assumption was more appropriate for small scales and small extents than for large scales and large extents. The reason is that the SARs were roughly linear in double logarithmic plot at small scales. The coefficients therefore did not change considerably. The actual variation of the coefficients K_{1-4} and FAE along the σ^* - axis produces the variation of observed points (diamonds) around the model (bold line) in Fig 3ab.